Proc. of 12th International Workshop on Positron and Positronium Chemistry, August 28–September 1, 2017, Lublin, Poland

A New Approach to the Presentation of the Positron Annihilation Lifetime Spectroscopy Results, *n*-Alkanes

B. Zgardzińska[a,*] and K. Standzikowski[b]

[a]Institute of Physics, Maria Curie-Skłodowska University, 20-031 Lublin, Poland

[b]Department of Geoecology and Palaeogeography, Maria Curie-Skłodowska University, 20-718 Lublin, Poland

The standard form of the positron annihilation lifetime spectroscopy results presentation are two plots of *o*-Ps lifetime and intensity as a function of external factor, e.g. temperature, pressure. Both *o*-Ps parameters change (stepwise) when in the medium phase transitions occur. For a more complete picture of the structural changes occurring in the matter we suggest to use an additional plot, in the coordinates, (τ_3, I_3). The hydrocarbons are selected to show the advantages following from the presentation of the results in the intensity–lifetime (INTI) plot.

DOI: 10.12693/APhysPolA.132.1496

PACS/topics: 36.10.Dr, 78.70.Bj, 82.30.Gg

1. Introduction

Positron studies of a medium are usually performed as a function of an external factor like temperature and pressure. The analysis of positron lifetime spectra gives us the values of *o*-Ps lifetime τ_{o-Ps} (τ_3), and its intensity I_{o-Ps} (I_3) (fraction of positrons forming *o*-Ps). The standard presentation of the positron annihilation lifetime spectroscopy (PALS) results is given in the form of two curves, τ_3 and I_3 as functions of external factor. We propose to present the results in the form of a curve in the coordinates (τ_3, I_3), with the changing factor as a parameter (the INTI plot — INtensity, lifeTIme) [1]. This kind of an approach is used sometimes in other positron studies, e.g. in the Doppler broadening spectroscopy [2–6], the results can be presented in (S, W) coordinates, or in AMOC [5, 6] form of presentation in (t, p) coordinates. In the literature one can find the papers that have already attempted to find a correlation between lifetime τ_{o-Ps} and intensity I_{o-Ps}, presenting the intensity as a function of free volume sizes [7].

The physicochemical processes taking place during the interaction of positrons and positronium with the matter influence the response produced at the PALS experiments. The spur model [8, 9] describing the Ps formation process assumes that high-energy positrons lose their energy by ionization processes and produce electrons, which can be trapped in the medium. These electrons enrich the reservoir of electrons, which can create the Ps atom with next positrons emitted from the source. Taking into account positron diffusion length and its lifetime in organic (small molecular) and polymer medium, one can conclude that some of the positrons can be localized before annihilation [10]. The studies performed with organic compounds and polymers [11–15] show that, as a consequence of these processes, the *o*-Ps intensity changes in time. The theoretical description of the nature of the electron and positron traps observed at low temperatures in the molecular medium, consistent with the experimental data, was proposed by Pietrow [16]. The experiments have shown that the exposure of samples to light eliminates the effects associated with e^- and e^+ trapping [13, 17]. The illumination does probably not affect other post-ionization products. In the liquid sample, the presence of paramagnetic oxygen molecules (dissolved in the sample) leads to the conversion of *o*-Ps into *p*-Ps. The conversion effect distorts the response obtained by the PALS technique in liquid samples, but is negligible in low temperature solid phases [18].

2. Experimental

The standard fast-slow positron annihilation lifetime spectrometer was used to measure lifetime spectra. The ^{22}Na positron sources (with an activity from 0.6 to 0.9 MBq) in the Kapton® envelope were located between two pieces of various samples in solid or liquid form. The statistics of each spectrum was better than 10^6 events. The LT v.9 program [19] was used to process the spectra, assuming three exponential decay components ascribed to: the *para*-positronium decay ($\tau_1 \approx 0.125$ ns); the annihilation of free positrons ($\tau_2 \approx 0.35$ ns) and the *ortho*-positronium decay ($\tau_3 > 0.9{-}3.5$ ns). At spectra analysis the constant ratio $I_{o-Ps} : I_{p-Ps} = 3 : 1$ was assumed.

The *n*-alkane samples (form Sigma Aldrich) have the purities better than 99%. Samples placed in the chamber were molten and degassed by freeze-thaw technique (to remove the paramagnetic oxygen molecules from the sample).

A general structural formula of *n*-alkanes is C_nH_{2n+2} (where n is the number of carbon atoms in the chain). The crystallographic structure of *n*-alkanes depends on the n number and is roughly correlated with parity of

*corresponding author; e-mail: bozena.zgardzinska@poczta.umcs.lublin.pl

the hydrocarbon chain. The n-alkanes appear in phases that can be classified as ordered or disordered ([1] and papers cited therein). The ordered crystalline phases (rigid, III, IV and V) and disordered phases (rotator RI, RII, RII, RIV) differ in the concentration of nonplanar conformers (mainly end-gauche, double-gauche, and kink conformers).

3. Results and discussion

3.1. The typical PALS results in n-alkanes

In hydrocarbons, the change of the PALS spectra parameters as a function of temperature occurs in a characteristic manner, allowing identification of phase and phase transition points. The n-alkanes with even number of carbon atoms $n < 22$ and odd with $n < 9$ show the presence of two phases only: rigid and liquid. The n-alkanes with the number n greater than that indicated above, show additional phase/phases (a rigid and/or rotator) before melting.

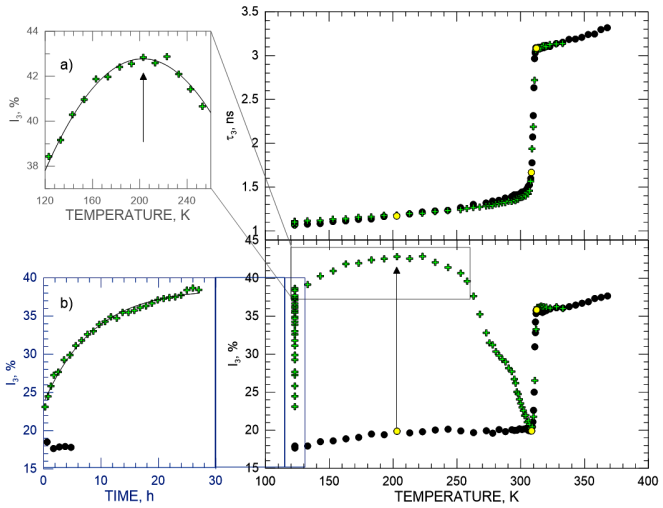

Fig. 1. The o-Ps lifetime (τ_3) and intensity (I_3) as a function of temperature in the n-eicosane (C20). Crosses — non-illuminated sample, dots — sample illuminated by $\lambda = 950$ nm, yellow circles — taken from Fig. 2. The inset (a) — magnified part of the plot $I_3(T)$ indicated by the frame. The inset (b) — the o-Ps intensity as a function of time at 123 K.

As an example of typical PALS results in n-alkanes, Fig. 1 shows the o-Ps parameters vs. temperature (T) in n-eicosane (C20). The sample was cooled from the room temperature to 123 K (during 40 min) and left at that temperature for 28 h. The o-Ps lifetime (τ_3) is stable at this temperature, but the o-Ps intensity (I_3) increases with time (inset (b)) if the sample is not illuminated. We observe the exponential increase of the o-Ps intensity — it reaches saturation after about 20 h. This effect is well known in the n-alkanes [20–22], their derivatives [23] and polymers [24, 25]. In the illuminated sample (here by $\lambda = 950$ nm) the o-Ps intensity has a low value ($\approx 17.5\%$) and does not change in time.

With an increase of temperature, the o-Ps parameters change. The τ_3 value does not depend on the illumination of the sample and increases with T, abruptly, at the phase transition rigid-liquid point. A similar character of the changes can be observed in I_3 in the illuminated sample. However, if the sample is not illuminated, in rigid phase the additional effects associated with sample irradiation by positrons — the consequence of e^- trapping effect is observed. At the temperature indicated by the arrow in Fig. 1, the I_3 reaches the maximum value (inset (a)), and with the further increase of T we observe a decrease of the o-Ps intensity (thermally induced detrapping effect). Just before the melting point, the I_3 reaches the minimum value (the same as in the illuminated sample). The effect was discussed in [26].

3.2. The INTI plot for n-alkanes

The changes of both PALS parameters (I_3 and τ_3) are correlated with the structural changes occurring in the sample with the change of temperature. Figure 2 shows

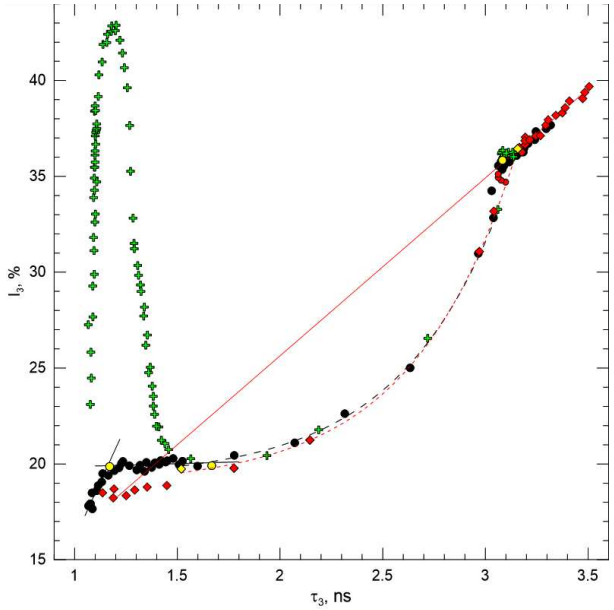

Fig. 2. The plot in the coordinates (τ_3, I_3) for n-eicosane (C20, crosses and dots) and n-decane (C10, diamonds) — INTI plot. Solid lines — fitted in three regions of (τ_3, I_3), correlated with the tendency of o-Ps parameters change; the line fitted in a liquid region is extrapolated to shorter lifetimes. Dashed line — the curve of the equation $I_3 - A = B\exp(C\tau_3)$, fitted in the points at phase transition rigid → liquid. Yellow circles and diamonds — points of line/curve intersection.

the changes of both o-Ps parameters. The INTI plot allows the precise determination of phase transition points and the study of the nature of structural changes. As one can see from Fig. 1, the history of the sample and measuring conditions (illumination/darkness) affects the results obtained by the PALS technique. In Fig. 2, the yellow circles indicate the characteristic points in the illuminated sample, at which the trends of (τ_3, I_3) are

changing. Between 123 and 203 K both *o*-Ps parameters increase, but above 203 K up to the melting point, we observe only the increase of the *o*-Ps lifetime. The first enhanced in Fig. 2 point (at 203 K) corresponds to the maximum value of *o*-Ps intensity in non-illuminated sample (see also the inset (a) in Fig. 1, the point marked by an arrow). In non-illuminated sample, this point separates the ranges of temperature for which an electron trapping and thermally induced emptying of traps effects are observed. It is important to mention that in the plots $\tau_3(T)$ and $I_3(T)$ it is difficult or impossible to determine this point. On the other hand, the presence of changes in the structure of organic media have been observed by other techniques, i.e. crystalline [27, 28] as well as amorphous [29]. Between the last point in rigid phase and the first one in the liquid phase (yellow dots in Figs. 1 and 2) the rigid → liquid phase transition occurs, when the *n*-eicosane crystal structure changes from the ordered triclinic to disordered structure. In this area, the difference between the sample illuminated and non-illuminated disappears. The points locate on the curve are given by the equation

$$I_3 - A = B\exp(C\tau_3), \tag{1}$$

where A, B, and C are 19.22%, 0.033, and 1.97, respectively. The *o*-Ps lifetime elongation by 1.6 ns corresponds to the *o*-Ps intensity growth by 14%. Although in the *n*-eicosane, the rotator phase was not detected, the correlated increase of both *o*-Ps parameters may correspond to a gradual increase in the concentration of conformers (characteristic for the rotator phase), finally reaching the total structural disorder of molecules in liquid phase. The presence of oxygen molecules in the sample interfere with the measured PALS parameters in the liquid, due to the *ortho–para* conversion. If the oxygen molecule is dissolved in the sample, the *o*-Ps lifetime remains constant (lower than in the degassed sample) with the increase of temperature (at range close to the melting point), although the growth of *o*-Ps intensity will be observed. The oxygen molecules penetrate the sample just at the beginning of the transition to the liquid state [18]. The presence of oxygen does not affect the estimated phase transition temperature, but interferes with the information about the size of the free volume.

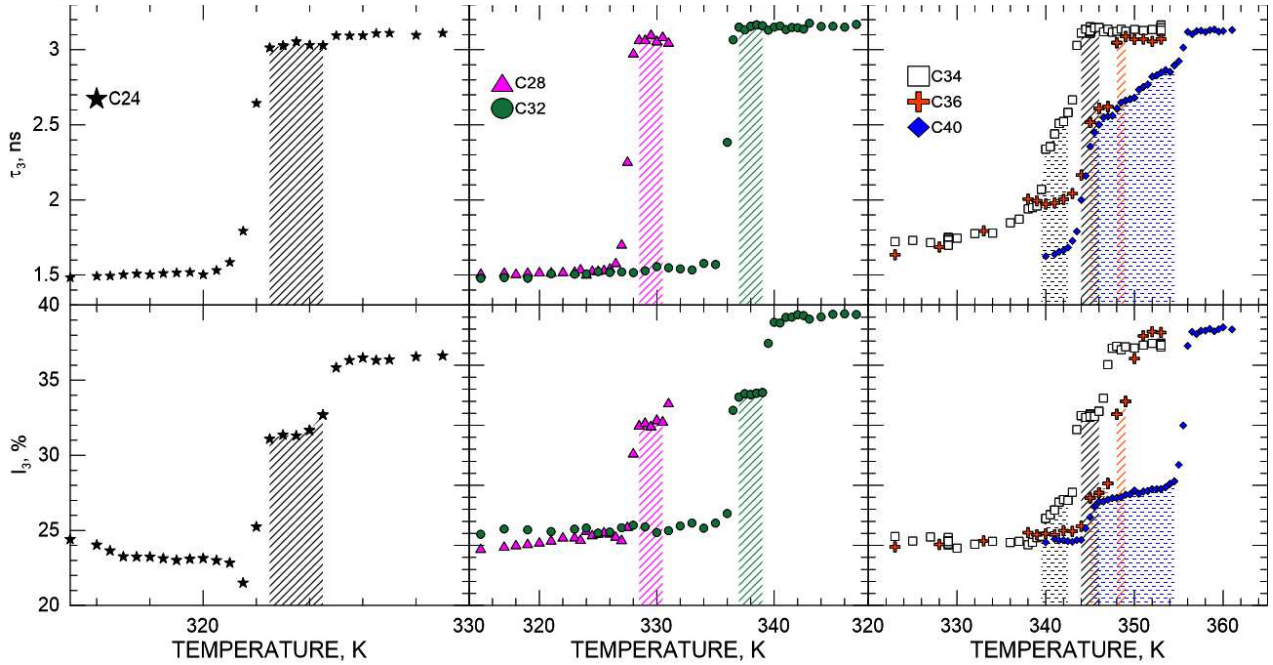

Fig. 3. The *o*-Ps lifetime (τ_3) and intensity (I_3) as a function of temperature in long-chain, even-numbered *n*-alkanes: $n = 24$ (stars), $n = 28$ (triangles), $n = 32$ (dots), $n = 34$ (squares), $n = 36$ (crosses) and $n = 40$ (diamonds). Slash marked areas correspond to the rotator phase, horizontally dashed areas — to the high temperature monoclinic phase.

The analysis of PALS results performed for other even-numbered *n*-alkanes with and without rotator phase/phases shows that all experimental points between ordered rigid phase and disordered liquid phase are arranged at the same curve given by Eq. (1) in the INTI plot. For *n*-decane (C10), the parameters A, B, and C in Eq. (1) are 18.86%, 0.034, and 1.97, respectively. The line fitted into the INTI plot dependence in liquid C10, extrapolated towards the lower values of the lifetime has the same directional coefficient (9.27) as the one fitted for C20. The analogies and similarities of the *o*-Ps lifetime as a function of the distance from the melting point in liquid *n*-alkanes with different chain length had been already discussed [30].

The PALS parameters (τ_3 and I_3) in *n*-tetracosane (C24) — the representative of even-numbered *n*-alkane with disordered rotator phase RII — change as it is shown in Fig. 3. As one can see (Fig. 4), above the rigid triclinic phase the points are arranged along the curve described by Eq. (1). All the points in the rotator phase (RII) are

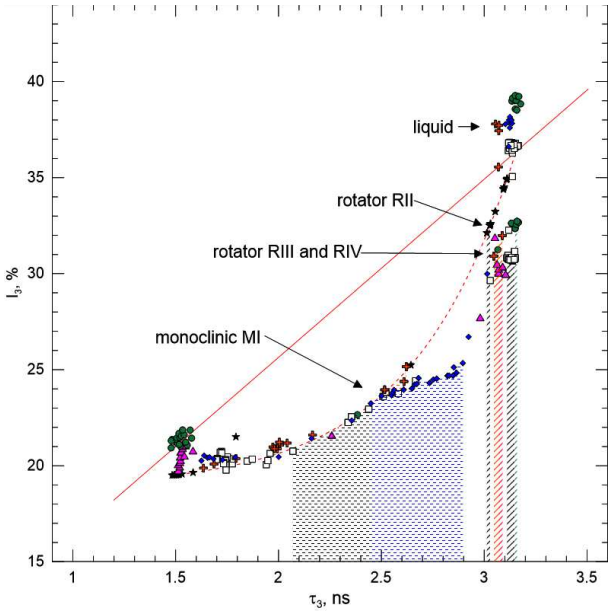

Fig. 4. The INTI plot for selected n-alkanes (points are described in Fig. 3). As a reference, the line and an exponential curve (dashed line) for C10 was added.

localized in the same area of the INTI plot — on the fitted (dashed) curve.

In the long-chain even-numbered paraffins (with $28 \leq n \leq 36$), the rotator phases (RIII and RIV) exist, while in n-alkanes with $n = 34$ and 36 also an additional ordered rigid (monoclinic) phase preceding the rotator phase can be observed (dashed areas in Figs. 3 and 4). In C28 and C32 presented in Fig. 3 the determination of the range of occurring of the rotator phase is possible only on the basis of the o-Ps intensity changes, because the o-Ps lifetimes in the rotator and liquid phases in long-chain n-alkanes with $n \leq 32$ are the same (≈ 3.1 ns). In the other n-alkanes presented in Fig. 3, C34 and C36, an additional rigid ordered phase exists, and both — the I_3 and the τ_3 — change during the phase transition ordered $\rightarrow$ disordered phase. In the last alkane presented in Fig. 3, n-tetracontane (C40), the melting point is preceded by ordered (high-temperature monoclinic MI) phase only, as it is suggested in the literature [31, 32], and the temperature range of this phase is marked in Fig. 3 by the dashed area.

The results for n-alkanes mentioned above (C28–C40) are shown in the INTI plot (Fig. 4). The points for o-Ps parameters in the rotator phase (RIII+RIV) are grouped in the region just below the exponential curve, regardless on the length of the hydrocarbon chain. The o-Ps parameters in a rigid ordered phase (monoclinic MI high ordered phase) in n-alkane with $n = 34$, 36 are arranged exactly along the line defined by the exponential curve. In the n-alkane without the rotator phase, C40, in the rigid pre-melting phase MI, the (τ_3, I_3) points lie below the exponential curve — the increase of o-Ps lifetime is significantly faster than the increase of o-Ps intensity. The rigid ordered phase seems to be the metastable phase preceding the rotator phase. This phase should manifest itself by an increase of the number of end-gauche conformers, while in the rotator phase the increase of concentration of kink type conformers should be observed [33, 34].

As the presented discussion indicates, in all n-alkanes having a triclinic structure, in the INTI plot the o-Ps parameters behave according to Eq. (1). The points ascribed to triclinic and monoclinic rotator phases (RIII and RIV) are located below the curve defined by Eq. (1).

Similar regular variations of PALS parameters in the INTI plot can be found for n-alkanes with an odd number of carbon atoms, they are summarized in paper [1]. As a consequence of the studies performed for the whole group of n-alkanes, the correlation between the crystalline structure and the position of τ_3 and I_3 points in the INTI graph was found (Fig. 5) [1]. The nature of the changes of the o-Ps parameters on the INTI plot, at the phase transition region, clearly corresponds to the crystal structure of n-alkanes. We want to emphasize that using the (τ_3, I_3) coordinates makes an identification of crystallographical structure of any n-alkane possible just on the basis of the localization of a single experimental point on the INTI plot (Fig. 5). In the even-numbered n-alkanes with the RI rotator phase the points representing the PALS results are arranged along the line fitted to the liquid phase region and extrapolated to lower I_3 and τ_3 values. In the n-alkanes with RII and RIII or RII+RIV rotator phases the PALS result points are arranged along the curve defined by Eq. (1) or below it. Such a differentiation of the rotator phases, as well as other phases, allows to specify the crystallographic structure based on the results obtained by the annihilation spectroscopy.

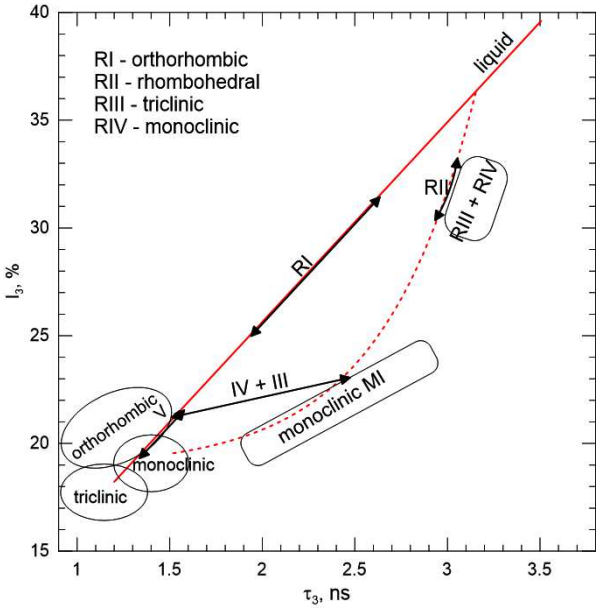

Fig. 5. The INTI plot for all n-alkanes showing the relationship with the crystallographic phases. The INTI plot is the map of crystallographic structure of n-alkanes.

4. Conclusions

The presentation of the PALS results as the plots in a newly proposed set of coordinates (τ_3, I_3) allows to expand the resource information obtained from the measurements carried out by this technique. It allows, among others, for:

1. More precise determination of phase transition points. Breakdown of trends on the (τ_3, I_3) plots corresponds to the phase transition points estimated in the figures $\tau_3(T)$ and $I_3(T)$.

2. Detection of the structural changes, which on the $\tau_3(T)$ and $I_3(T)$ plots are negligible or unidentifiable. The scale of I_3 and τ_3 changes as a function of temperature sometimes is too small, so they cannot be treated as the structural ones. However, the mutual changes of these parameters clearly indicate a change in positronium interactions with the matter.

3. Determination of the nature of the changes taking place in the phase transition area.

4. Unification of the results for the group of compounds having the same or similar structural construction; the nature of the changes in the INTI plot is the same, and an estimation of crystallographic structure is possible.

Acknowledgments

The authors would like to thank Prof. Tomasz Goworek for helpful discussions during the preparation of the manuscript and for the first review of this article.

References

[1] B. Zgardzińska, K. Standzikowski, *Phys. Rev. Lett.*, 2017, submitted for publication.

[2] L.C. Smedskjaer, M.J. Fluss, D.G. Legnini, *Nucl. Instrum. Methods Phys. Res. B* **4**, 196 (1984).

[3] D.T. Britton, A. van Veen, *Nucl. Instrum. Methods Phys. Res. A* **275**, 387 (1989).

[4] S. Mantl, W. Triftshäuser, *Phys. Rev. B* **17**, 1645 (1978).

[5] O.E. Mogensen, *Positron Annihilation in Chemistry*, Springer-Verlag, 1995, Ch. 3.

[6] D.M. Shrader, Y.C. Yean, *Positron and Positronium Chemistry*, Elsevier, 1988, Ch. 3.

[7] G. Roudaut, G. Duplâtre, *Phys. Chem. Chem. Phys.* **11**, 9556 (2009).

[8] O.E. Mogensen, *J. Chem. Phys.* **60**, 998 (1974).

[9] S.V. Stepanov, V.M. Byakov, *J. Chem. Phys.* **116**, 6178 (2002).

[10] T. Hirade, N. Suzuki, F. Saito, T. Hyodo, *Phys. Status Solidi C* **4**, 3714 (2007).

[11] T. Suzuki, T. Miura, Y. Oki, M. Numajiri, K. Kondo, Y. Ito, *J. Phys. IV* **3**, 283 (1993).

[12] C.L. Wang, T. Hirade, F.H.J. Maurer, M. Eldrup, N.J. Pedersen, *J. Chem. Phys.* **108**, 4654 (1998).

[13] T. Hirade, F.H.J. Maurer, M. Eldrup, *Radiat. Phys. Chem.* **58**, 465 (2000).

[14] T. Goworek, R. Zaleski, J. Wawryszczuk, *Chem. Phys.* **295**, 243 (2003).

[15] T. Goworek, J. Wawryszczuk, R. Zaleski, B. Zgardzińska, *Radiat. Phys. Chem.* **76**, 185 (2007).

[16] M. Pietrow, *Phys. Chem. Chem. Phys.* **17**, 27726 (2015).

[17] T. Hirade, C.L. Wang, F.H.J. Maurer, M. Eldrup, N.J. Pedersen, in: *Abstract Book for 35th Annual Meeting on Radioisotopes in the Physical Science and Industries, Tokyo*, 1998, p. 89.

[18] B. Zgardzińska, W. Białko, B. Jasińska, *Nukleonika* **60**, 801 (2015).

[19] J. Kansy, *Nucl. Instrum. Methods Phys. Res. A* **374**, 235 (1996).

[20] M. Pietrow, J. Wawryszczuk, *Mater. Sci. Forum* **733**, 75 (2013).

[21] M. Pietrow, J. Wawryszczuk, *Mater. Sci. Forum* **666**, 89 (2011).

[22] M. Pietrow, J. Wawryszczuk, *Nukleonika* **55**, 51 (2010).

[23] T. Suzuki, R.S. Yu, V.P. Shantarovich, Y. Ito, K. Kondo, *Phys. Status Solidi C* **4**, 3706 (2007).

[24] Z.L. Peng, B.G. Olson, J.D. McGervey, A.M. Jamieson, *Polymer* **40**, 3033 (1999).

[25] Y. Kobayashi, W. Zheng, E.F. Meyer, J.D. McGervey, A.M. Jamieson, R. Simha, *Macromolecules* **22**, 2302 (1989).

[26] B. Zgardzińska, T. Hirade, T. Goworek, *Chem. Phys. Lett.* **446**, 309 (2007).

[27] M. Lukesova, B. Zgardzinska, H. Svajdlenkova, R. Zaleski, B. Charmas, J. Bartos, *Physica B Condens. Matter* **476**, 100 (2015).

[28] J. Bartos, H. Svajdlenkova, R. Zaleski, M. Edelmann, M. Lukesova, *Physica B Condens. Matter* **430**, 99 (2013).

[29] H. Švajdlenková, O. Šauša, M. Iskrová-Miklošovičová, V. Majerník, J. Krištiak, J. Bartoš, *Chem. Phys. Lett.* **39**, 539 (2012).

[30] B. Zgardzińska, T. Goworek, *Chem. Phys.* **405**, 32 (2012).

[31] S. Wang, K.-I. Tozaki, H. Hayashi, H. Yamamoto, *Therm. Acta* **448**, 73 (2006).

[32] H. Kubota, F. Kaneko, T. Kawaguchi, M. Kawasaki, *J. Chem. Phys.* **121**, 1121 (2004).

[33] M. Maroncelli, S.P. Qi, H.L. Strauss, R.G. Snyder, *J. Am. Soc.* **104**, 6237 (1982).

[34] M. Maroncelli, H.L. Strauss, R.G. Snyder, *J. Chem. Phys.* **82**, 2811 (1985).